Est. 1984

ORIENTAL JOURNAL OF CHEMISTRY
An International Open Access, Peer Reviewed Research Journal

www.orientjchem.org

ISSN: 0970-020 X
CODEN: OJCHEG
2023, Vol. 39, No.(4):
Pg. 904-912

Fabrication and Electrochemical Investigation of RGO-NiO Nanocomposite Electrodes for Supercapacitor Applications

ASA PALAKKADEN SUBRAMANIAN[1], ANITHA KUMARY VIDYADHARAN[1]*, and CHITHRA POOMALA GOPI[1]

[1]Department of Chemistry, Sree Narayana College for Women Kollam, India.
*Corresponding author E-mail: anithasreevalsan@gmail.com

http://dx.doi.org/10.13005/ojc/390411

(Received: June 08, 2023; Accepted: July 20, 2023)

ABSTRACT

The present investigation details the hydrothermal production of RGO-NiO nanocomposite and examines the electrochemical performance of the composite electrode functioning on an adaptable carbon cloth substrate. The RGO-NiO nanostructures display incredible super-capacitive functionality when used in a two-electrode system with a 2 M KOH-PVA electrolyte. This is due to the unique characteristics of RGO, which functions as a flexible and expandable platform for creating NiO nanocrystals with a nanoscopic spherical morphology. Large surface areas in these nanostructures facilitate ion diffusion, which ultimately raises specific capacitance. The nanocomposite electrode as-prepared displays a robust two-electrode structure, a constant potential window between (0V and 0.45V), and specific capacitances of up to 749F/g from CV at a rate of scan of 5mV/s and 366F/g from GCD at 1A/g. 5000 cycles of cyclic stability were examined, and the capacitance retention was 91.23% after successive cycles.

Keyword: Electrochemical, RGO-NiO nanocomposite, Supercapacitor.

INTRODUCTION

Since energy is a necessity for survival, devices with large energy storage capacities are the immediate requirement for any developing country[1]. The life span of natural sources of energy is the main challenge to be addressed to meet our needs. As a result, batteries and supercapacitors are crucial for achieving these goals. Between electrolytic capacitors and batteries, they serve as an intriguing transitional device that can store energy in the form of charges[2]. Charges accumulate in the conducting contact between the electrode and electrolyte rather than on the surface[3]. The electrode material has a considerable impact on supercapacitor performance. The size of the pores of the conducting materials, which can be changed by the straightforward addition of nanostructures, determines the electrochemically active surface area[4]. Carbon-based materials, like active carbon, CNTs, and graphene-based are frequently employed as supercapacitor electrodes because of their stability, excellent conductivity, and broad surface area[5]. Graphene by virtue of its surface area is the most attractive material compared to any other carbon materials. It also offers a variety of other properties that make it ideal for supercapacitors,

including as outstanding electrical and thermal conductivity, light weight, and high chemical stability[6]. Studies have shown that creating reduced graphene oxide from graphene oxide lowered the amount of water present while maintaining the beneficial gas permeability properties[7]. Metal oxides can be utilized to make electrodes because they have a high specific capacitance[8]. In the majority of pertinent studies, ruthenium oxide has been explored but it is expensive and many alternatives such as manganese and ferrous oxides, are being studied for use as supercapacitor electrodes[9]. Because of their beneficial synergistic effects, porous carbon materials are frequently utilized with electro-active materials that show pseudo-capacitance to increase the total capacitance of the electrode materials. Numerous investigations have looked into how well NiO-based supercapacitors perform electrochemically.[10]

A variety of synthetic procedures have been used by various researchers to increase the effectiveness of these materials. To improve the materials' electrical conductivity and match the power density of metal oxide-based pseudo capacitors, RGO has recently been doped with metal oxides and metal oxide nanocomposites. It has been found that composite materials with carbonaceous components like GO and RGO increase the specific capacitance and longevity of supercapacitors[11]. Yu-Lung Shih *et al.,* created an all-solid-state, asymmetric SC that is built on Ni_2P/RGO/NiO/NF electrodes and was effective in turning on a light-emitting diode[12]. According to Padmanabhan *et al.,*[13], in order to create a 3D hierarchical nanohybrid with a specific energy density of 19.4 Wh/Kg at a high-power density of 1003 W/Kg, NiO nanoflakes and nanoflowers were attached to carbon fiber fabric. Ao Liu and colleagues have successfully created an asymmetric supercapacitor utilizing RGO and honeycomb-like NiO[14]. The asymmetric supercapacitor excels in performance and can light an LED thanks to its 74.4 F g^{-1} specific capacitance, 23.25 Wh kg^{-1} energy density, and 9.3 kW kg^{-1} power density. A two-electrode configuration uses less electrolyte solution, which stops the supercapacitor from leaking and enables the production of supercapacitors at a reasonable price. The creation of sandwich NiO/RGO nanohybrids is described in this work using the hydrothermal reduction of porous hetero-assembled $Ni(OH)_2$/RGO. To identify the underlying relationships, the electrochemical performance was thoroughly studied in connection to the microstructural features of the nanohybrids.

The hydrothermal development of RGO-NiO nanocomposite is described in this paper, along with an analysis of the composite's electrode performance in supercapacitor applications. With the use of several characterization techniques, the composite was analyzed. Electrochemical techniques such as CV, GCD, and impedance were used to investigate electrode performance.

MATERIALS AND METHODS

Materials

Nickel nitrate hexahydrate (Ni $(NO_3)_2.6H_2O$, natural graphite flakes (–10 mesh, 99.9%), sulfuric acid (H_2SO_4, 95%) and potassium permanganate ($KMnO_4$, 99%) ,Phosphoric acid (H_3PO_4, 85%), hydrogen peroxide (H_2O_2, 30%), and hydrochloric acid (HCl) were purchased from Sigma-Aldrich. For the electrochemical performance evaluations, the electrolyte solution was made using potassium hydroxide (KOH, Merck). H_2SO_4 and H_2O_2 MERCK and ultra-pure water were used as solvents throughout the study.

Synthesis of Graphene oxide (GO)

In a typical procedure, pure graphite powder was used to produce graphene oxide (GO) by the modified Hummers method[15]. The initial stage involves combining and stirring sulfuric acid (H_2SO_4) and phosphoric acid in a 9:1 volume ratio. 1 g of graphite powder was carefully introduced in dropwise addition to the combined solution. After 12 h of stirring, the solution had turned dark green. The mixture was rapidly agitated and $KMnO_4$ (6 g) was slowly added, limiting the temperature below 20°C. The mixture was then stirred for 18 h in a water bath at 35°C. 2 mL of H_2O_2 was progressively added and shaken for 10 min to remove the excess $KMnO_4$. To this dropwise addition of 150 mL of distilled water was done to maintain adequate temperature. Later washing of the mixture was carried out with sufficient amount of deionized water and HCl. GO suspension was created by ultrasonicating graphite oxide for an hour.

Preparation of RGO-NiO nanocomposites

1.95 gram of nickel nitrate hexahydrate was dissolved in 10 mL of ethylene glycol and

100 mL of DI water to form a 0.5 M Ni^{2+} precursor solution. To achieve a pH of 8, the required amount of 30% ammonium hydroxide (NH_4OH) was applied. The mixture was mixed using an ultrasonicator for an hour while being constantly agitated to assist hydrolysis, esterification, polyesterification, and gel formation[16]. The solution is now combined with ultrasonically diluted GO dispersion. Mother liquor-containing amorphous precipitates were placed in a stainless steel autoclave and treated for 24 h at 170°C. The suspension was hydrothermally treated, centrifuged, powdered, washed with deionized water, dried for another 12 h at 90°C, and finally calcined for three hours at 150°C. For comparison, pure NiO was synthesized using the same hydrothermal and sol-gel processes but without the inclusion of graphene oxide. To ascertain the impact of graphene content on electrochemical characteristics, samples made of GO and NiO nanosheets with initial mass ratios of 50:50 were created.

Characterization techniques

The structure of GO, RGO, and RGO-NiO was investigated using FESEM with EDAX and HRTEM (JEOL JEM-2100 microscope at 200 kv). GO, RGO, NiO, and RGO-NiO phase composition investigations were analyzed utilizing X-ray diffraction (XRD) technology. In addition to using XRD, samples were analyzed using a FT Raman Spectrometer (Thermo Scientific DXR Raman spectrometer with a 532-wavelength laser). The FTIR (Fourier transform infrared spectroscopy) data for the GO, RGO, NiO, and RGO-NiO were obtained using a FTIR spectrometer. Using XPS (X-ray photoelectron spectroscopy), the chemical composition and bonding states of RGO, NiO, and RGO-NiO were investigated.

Electrochemical measurements

The carbon fabric was divided into pieces of 1 cm^2 by 1 cm^2. In order to remove any grease, dust, or other material from the surface of the bare carbon cloth (bare CC), acetone, ethanol, and distilled water were used to clean it under ultrasonication for more than 10 minutes. The naked CC was subjected to a 30-min sonication in concentrated nitric acid in order to graft carboxyl and hydroxyl active functional groups onto the surface. The naked CC was then dried in an oven at 60°C after being rinsed ultrasonically for 10 min in each of 100% ethanol and distilled water, respectively. Pre-treated carbon clothing (pre-treated CC) was produced by repeating this method twice.

A homogeneous combination of the analyte, PVDF, and carbon black was treated in 3 mL of NMP at a mass ratio of 70:15:15 to produce a liquid slurry. The slurry was applied to a carbon cloth surface using a drop casting process. To begin, a homogeneous coating is applied and left to dry. In a similar fashion, double coating was applied. Each electrode's active substance was sandwiched atop an electrolyte layer, and the two symmetrical electrodes would be filled with around 0.6 mg. The constructed supercapacitor was fully sealed after attaching leads to the two electrodes for external contact. Carbon cloth was used to soak the electrolyte. The two electrodes are put face to face with a separator in between as a buffer and sealed. The electrochemical measurements of the two-electrode cell were analyzed by cyclic voltammetry CV, galvanostatic charge–discharge and EIS using Zahneer Zennium Pro Electrochemical workstation The following equations were used for electrochemical analysis in the study.

$$Csp=\int IdV/\nu m\Delta V \quad (1)$$

Where "m" stands for the mass of the loading on the working electrode, "v" stands for the scan rate in V/s, and "V" is the potential window (V) of the CV measurement.

$$Csp=\int I\Delta t/m\Delta V \quad (2)$$

Where 'm' is the mass loading on the working electrode, 'I' is the current (A), 't' is the discharge time (s), and 'I' is the current (A). The charge-discharge window is denoted by (V). The following formulae were used to compute the specific energy (E) in Wh/Kg and the specific power (P) in W/Kg.

$$E = \frac{0.5Csp(\Delta V)^2}{3.6} \quad (3)$$

$$P = E * \frac{3600}{\Delta t} \quad (4)$$

RESULTS AND DISCUSSION

X-ray Diffraction Analysis

X-ray diffraction spectra of the RGO-NiO composite is depicted in Fig. 1 with NiO peaks

inset. According to JCPDS No. 47-1049[17], the distinctive NiO diffraction peaks were found at 2theta values of 33.72° and 60.02°, which correspond to the lattice planes (111) and (012), respectively. Effective reduction of GO to RGO is evident from the diffraction peaks from the (002) plane of GO at 11° which is displaced to 26° of RGO. The decrease in RGO peak intensity and crystallinity indicates that the amorphous NiO has successfully integrated with the RGO. This integration is likely to improve the features of the composite, such as its electrical conductivity and stability.

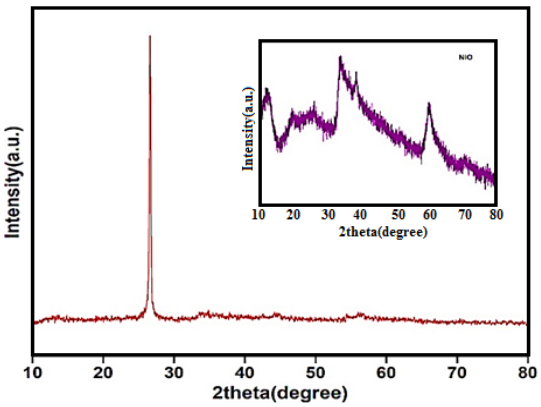

Fig. 1. X-ray diffraction spectra of RGO-NiO Composite (Inset: XRD spectra of NiO)

SEM and TEM Analysis

SEM and EDAX elemental mapping were used to study the morphology and chemical composition of the samples. Fig. 2 (A-C) shows SEM micrographs of synthesized RGO, NiO, and RGO-NiO composite samples. NiO has nearly spherical and RGO had the typical sheet-like morphology. The composite samples reveal a homogeneous distribution of NiO in the RGO matrix. The homogenous distribution of NiO in the RGO matrix can improve the composite material's conductivity and mechanical properties.

EDAX profile of the prepared materials are illustrated in Fig. 2(D-F). Peak lines in the spectra are seen at 0.56 keV and 0.28 keV, respectively, which correspond to the Ka elemental spots of oxygen and carbon in RGO (%C:92.10, %O:7.90). The typical La and Ka elemental spots of nickel in NiO samples are located at energies of 0.85 KeV and 7.47 keV, respectively (%Ni: 64.08, %O:35.92). Additionally, oxygen's distinctive elemental peak is present. The RGO-NiO composite sample contains all the aforementioned elemental peaks, proving that the composite has successfully evolved (%C:71.23, %O:14.39, %Ni:14.38).

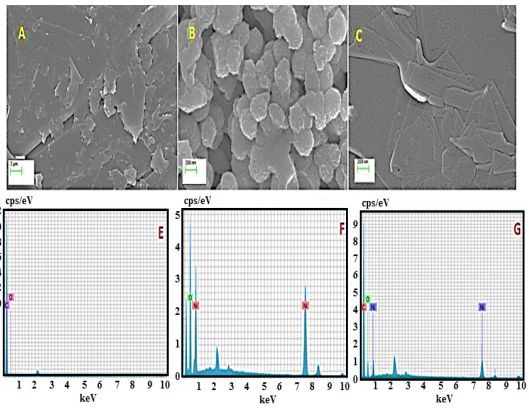

Fig. 2. FESEM micrographs of A) RGO, B) NiO, C) RGO-NiO Composite, EDAX profile of D) RGO, E) NiO, and F) RGO-NiO composite

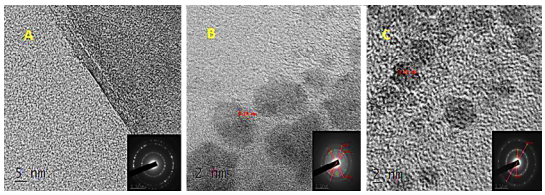

Fig. 3. HRTEM images of A) RGO, B) NiO, and C) RGO-NiO composite (Inset: corresponding SAED patterns)

Figure 3 shows HRTEM images of synthesized nano materials. The SEM observations of sheet-like RGO and near-spherical NiO morphology are confirmed by the micrographs. The average dimension of NiO nanoparticles was found to be ~8nm. The distinctive SAED patterns, which are shown as an inset to the HRTEM images, are in good agreement with the accepted diffractions JCPDS No. 47-1049. SAED patterns of RGO were observed as crystalline, as observed in the XRD examination, and it was greatly reduced with the integration of NiO nanoparticles.

Infrared Spectra Analysis

Figure 4 represents the FTIR spectra of the samples produced. The spectra of NiO nanoparticles show the characteristic Ni-O and Ni-O-Ni stretching vibrations at 630 and 1080 cm^{-1} respectively. Additionally, the peaks that appeared at 3043 and 1640 cm^{-1} are attributed to O-H stretching and bending of absorbed water molecules. The existing peak at 1398 cm^{-1} is connected to the N=O stretching frequency generated by a trace quantity of nitrate.

The spectra of RGO show peaks at 3436, 1631, 1385, 1056, 2923, 2838, 1250 and 801 cm^{-1}, which correspond to OH stretching, C=C stretching in sp^2 carbons, O–H bending vibration, C–O stretching, -CH_2 stretching, C-O-C bond, and C-H bending, respectively. The FTIR spectrum of the RGO-NiO composite shows Ni-O stretching vibrations as well as RGO-specific vibrations. The oxygen-containing RGO functions were visible at altered wavenumbers, proving the effective formation of the RGO-NiO composite.

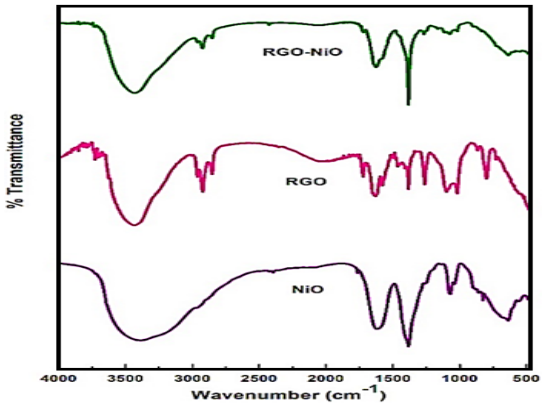

Fig. 4. FTIR spectra of RGO, NiO and RGO-NiO composite

Raman Analysis

The Raman scattering of the samples is depicted in Fig. 5. The RGO G and D bands, which are depicted as disorder and tangential bonds[17], correlate to the two different peaks at 1344 and 1577 cm^{-1}. Significant intensity peaks at 486, 728, 870 and 1050 cm^{-1} attributed to NiO vibrational modes with LO, 2TO, LO+LO, and 2LO, respectively. The composite Raman spectra reveal distinct NiO (LO, and 2TO vibrations) and RGO (G and D bands) peaks, confirming the successful synthesis of RGO-NiO.

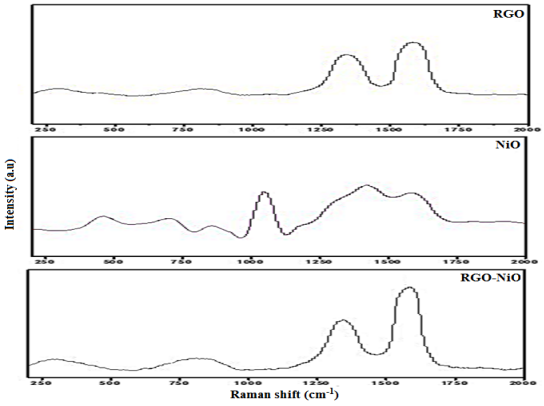

Fig. 5. FT Raman spectra of RGO, NiO, and RGO-NiO composite

XPS Analysis

The surface chemical states, composition change, and interaction of nanocomposites were examined using XPS. The C1s peak for RGO, NiO, and RGO-NiO composite appeared around 284.6 eV. The O1s peak is found at 529.8, 530.1 and 530.2 eV for RGO, NiO, and RGO-NiO accordingly[18]. The existence of RGO, NiO, in RGO-NiO hybrids was confirmed from the survey scan of RGO-NiO composite surface. The shift towards higher binding energy for the composite material rises from the interaction of NiO on RGO matrix.

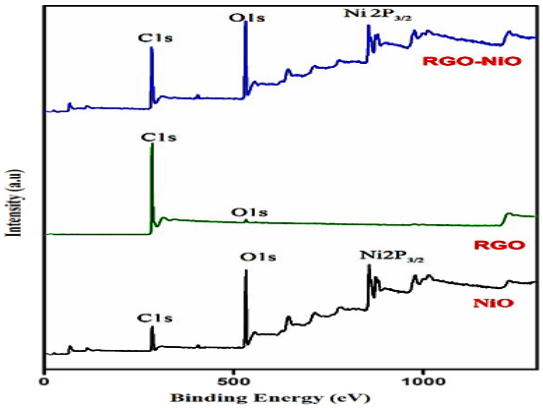

Fig. 6. XPS survey survey scan profile of RGO, NiO, and RGO-NiO composite

Electrochemical Evaluation

Cyclic Voltammetry

Three electrode systems were used to assess the electrochemical characteristics of RGO-NiO nanocomposites. Fig. 7. A depicts the cyclic voltammetry (CV) curves obtained for the composite in 2M KOH electrolyte with a potential range of 0-0.45V at different scan rates. Because of the electrochemical double layer capacitor (EDLC) process, the RGO nanosheets had the lowest current density response. Due to the reversible redox reaction of NiO (Ni^{2+}/Ni^{3+}), the faradaic reaction of NiO in an alkaline electrolyte was shown to give little specific capacity during electrochemical processes. In comparison to pure materials, the composite electrode enhances the contact surface area, resulting in faster ion diffusion and faradaic response. Furthermore, the combination of RGO sheets with NiO nanoparticles can significantly improve electronic transmission. The redox reaction of hydroxyl ions and NiO in alkaline media produced the CV curves shown. This reversible reduction procedure can be described as follows:

$$Ni(OH)_2 + OH \leftrightarrows Ni(OOH) + H_2O + e^- \quad (5)$$

The superior capacitance and decreased contact resistance of the NiO-RGO nanohybrids in the presence of KOH electrolyte have been shown to make them a potential candidates for energy storage. This behavior is further demonstrated by the fact that the nanohybrids' symmetry redox form does not change even when the potential scan rate is increased to 100 mV/s in the voltage range of 0.0 to 0.45 V. The specific capacitances (Csp) of the RGO-NiO electrode were calculated using CV measurements and were found to be 749F/g at a scan rate of 5mV/s. In figure 7.B, the Csp values at different scan rates are shown.

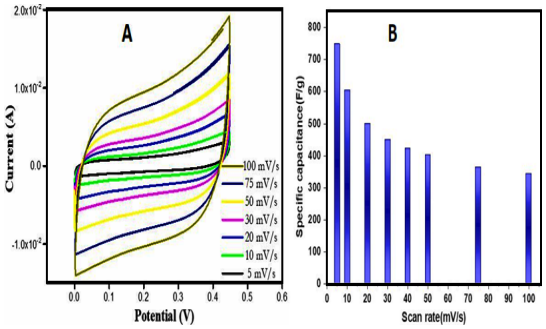

Fig. 7. Cyclic voltammetry curves of various RGO-NiO

GCD Analysis

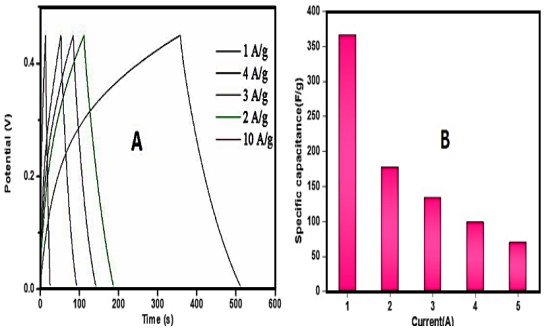

Fig. 8A. GCD curve of RGO-NiO composites at varying current densities B) specific capacitance of composite electrode vs current density

Figure 8A depicts the GCD performance of the RGO-NiO composite at varying current densities. In the tested current densities, a typical triangle-type charge discharge profile was achieved for the electrode, which is typical of an ideal supercapacitor electrode. Furthermore, the charge-discharge period increases with decreasing current density (Fig. 8B) due to hydroxyl radical insertion/exertion during the electrochemical process. The maximum storage capacity, Csp of 366F/g was obtained for the composite electrode at 1A/g.

Electrochemical Impedance Spectra

To comprehend the charge transfer/ diffusion mechanisms in the electrode-electrolyte interface, EIS measurements were carried out. Fig. 9 depicts the results of EIS spectra as Nyquist plots. The Nyquist plot was fitted to an equivalent circuit consisting of the components R_{ct}, Equivalent series resistance and constant phase element (CPE; 1), and ZW (see Fig. 9 inset). R_{ct} and ESR were calculated to be 1.5 and 0.2, respectively. The Nyquist plots in the high-frequency region show a modest semicircular loop linked with the charge transfer resistance (R_{ct}), indicating a low internal resistance of the electrode[19]. The Warburg impedance (ZW), which is connected to the ionic diffusion resistance was observed in the low-frequency scan on the Nyquist plots as a virtually straight line parallel to the Y axis. The Warburg line in the low-frequency area of the RGO-NiO composite electrode becomes a more vertical, straight line due to the faster ion diffusion, exhibiting anticipated capacitive behavior.

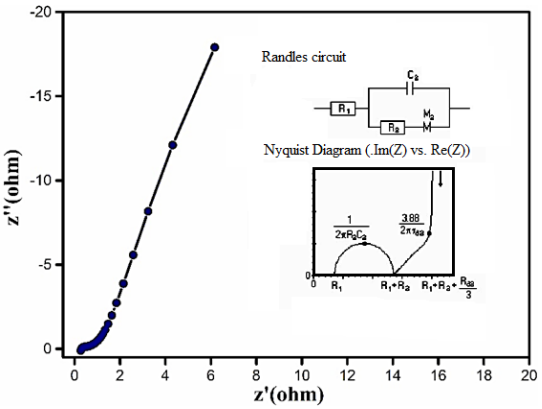

Fig. 9. EIS analysis of RGO, NiO and RGO-NiO composite electrodes. Inset figure represents high frequency data

Cyclic Stability

The cycle stability of nanocomposite electrode was studied for 5000 consecutive cycles at 8A/g. Fig. 10 shows the cyclic stability and percentage capacitance retention of the

sample. After 5000 continuous cycles, 91.23% specific capacitance was preserved. The findings demonstrate the RGO-NiO composite electrode's high cycle stability and potential for usage in energy storage systems. The RGO 2-D sheet structure and close coupling of RGO-NiO composite material give great cycle stability and quicker electron/ion transition. Future investigations are planned in terms of long-term stability under varied operating conditions to investigate the material's practical application. Table 1 displays a comparison between the synthesized composite material with other similar studies revealing the superior performance of the prepared RGO-NiO composite material.

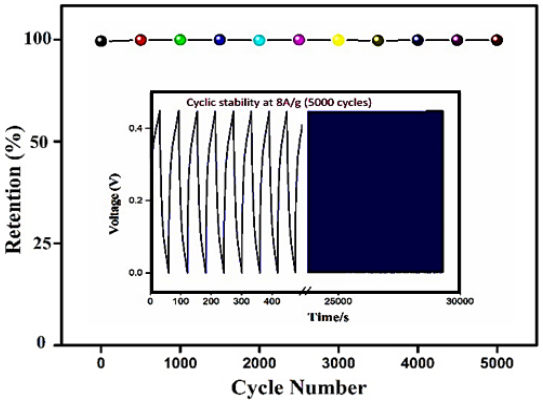

Fig. 10. Percentage capacitance retention of RGO-NiO composite electrode for 5000 consecutive cycles (Inset: GCD curves)

Table 1: Comparison of current study with existing reports

Working electrode	Current collector	Electrolyte	Scan rate/current density	Specific capacitance(F/g)	Reference
RGO/NiO	Nickel Foam	6M KOH	0.38A/g	428	20
2DrGO/NiO	ITO glass	1M KOH	0.5mA cm^{-2}	269	21
$Ni(OH)_2$/graphene	Nickel foam	6M KOH	1mV s^{-1}	218.4	22
RGO/NiO	Carbon cloth	2M PVA-KOH	1A/g	366	Current work

CONCLUSION

In conclusion, we successfully synthesized 2-dimensional Reduced Graphene Oxide-Nickel Oxide nanohybrid materials for use as electrodes in supercapacitors. The composite electrode displays remarkable electrochemical characteristics due to the uniformly dispersed NiO and graphene nanosheets as well as the strong bonding of NiO nanosheets and graphene. These characteristics have been proven to exhibit excellent stability, delivering consistent performance over time. The Csp value of a composite with a 50:50 percentage of RGO and NiO was determined to be 749 F/g from CV and 366 F/g from GCD, with an outstanding cyclic stability of 91.23%.

ACKNOWLEDGMENT

The authors acknowledge the service and help given by the Advanced Research Centre, Department of chemistry, Calicut University of and Institute of Advanced Studies PSG, Coimbatore for providing the facilities for the current study. CLIF, Kerala University for XPS analysis, DST-SAIF Cochin, India for carrying out FTIR, TEM, SEM-EDAX, XRD and RAMAN analyses.

Conflict of Interest

The authors state that they donot have any known competing financial interests, personal ties to affect the work reported in this study.

REFERENCE

1. (a) Conte, M., Supercapacitors technical requirements for new applications. *Fuel cells.,* **2010**, *10*(5), 806-818; (b) Denholm, P.; Ela, E.; Kirby, B.; Milligan, M. Role of energy storage with renewable electricity generation; National Renewable Energy Lab.(NREL), Golden, CO (United States): 2010; (c) Divya, K.; Østergaard, J., Battery energy storage technology for power systems-An overview. *Electric power systems research*., **2009**, *79* (4), 511-520.
2. Sharma, P.; Kumar, V., Current technology of supercapacitors: A review. *Journal of Electronic Materials.,* **2020**, *49*(6), 3520-3532.
3. (a) Beidaghi, M.; Gogotsi, Y., Capacitive energy storage in micro-scale devices: recent advances in design and fabrication of micro-supercapacitors. *Energy & Environmental Science*., **2014**, *7*(3), 867-884; (b) González, A.; Goikolea, E.; Barrena, J. A.; Mysyk, R., Review on supercapacitors: Technologies and materials. *Renewable and sustainable energy reviews*., **2016**, *58*, 1189-1206.

4. (a) Wang, G.; Zhang, L.; Zhang, J., A review of electrode materials for electrochemical supercapacitors. *Chemical Society Reviews.,* **2012**, *41*(2), 797-828; (b) Wei, W.; Cui, X.; Chen, W.; Ivey, D. G., Manganese oxide-based materials as electrochemical supercapacitor electrodes. *Chemical society reviews.,* **2011**, *40*(3), 1697-1721; (c) Zhang, L. L.; Zhao, X., Carbon-based materials as supercapacitor electrodes. *Chemical Society Reviews*., **2009**, *38*(9), 2520-2531.
5. Zhai, Y.; Dou, Y.; Zhao, D.; Fulvio, P. F.; Mayes, R. T.; Dai, S., Carbon materials for chemical capacitive energy storage. *Advanced materials*., **2011**, *23*(42), 4828-4850.
6. Zhu, Y.; Murali, S.; Stoller, M. D.; Ganesh, K. J.; Cai, W.; Ferreira, P. J.; Pirkle, A.; Wallace, R. M.; Cychosz, K. A.; Thommes, M., Carbon-based supercapacitors produced by activation of graphene. *Science*., **2011**, *332* (6037), 1537-1541.
7. Smith, A. T.; LaChance, A. M.; Zeng, S.; Liu, B.; Sun, L., Synthesis, properties, and applications of graphene oxide/reduced graphene oxide and their nanocomposites. *Nano Materials Science*., **2019**, *1*(1), 31-47.
8. Jiang, J.; Li, Y.; Liu, J.; Huang, X.; Yuan, C.; Lou, X. W., Recent advances in metal oxide-based electrode architecture design for electrochemical energy storage. *Advanced materials*., **2012**, *24*(38), 5166-5180.
9. Fang, Y.; Zhang, Q.; Cui, L., Recent progress of mesoporous materials for high performance supercapacitors. *Microporous and Mesoporous Materials*., **2021**, *314*, 110870.
10. Chime, U. K.; Nkele, A. C.; Ezugwu, S.; Nwanya, A. C.; Shinde, N.; Kebede, M.; Ejikeme, P. M.; Maaza, M.; Ezema, F. I., Recent progress in nickel oxide-based electrodes for high-performance supercapacitors. *Current Opinion in Electrochemistry*., **2020**, *21*, 175-181.
11. (a) An, C.; Zhang, Y.; Guo, H.; Wang, Y., Metal oxide-based supercapacitors: progress and prospectives. *Nanoscale Advances*., **2019**, *1* (12), 4644-4658; (b) Delbari, S. A.; Ghadimi, L. S.; Hadi, R.; Farhoudian, S.; Nedaei, M.; Babapoor, A.; Namini, A. S.; Van Le, Q.; Shokouhimehr, M.; Asl, M. S., Transition metal oxide-based electrode materials for flexible supercapacitors: A review. *Journal of Alloys and Compounds*., **2021**, *857*, 158281; (c) Sayyed, S. G.; Mahadik, M. A.; Shaikh, A. V.; Jang, J. S.; Pathan, H. M., Nano-metal oxide based supercapacitor via electrochemical deposition. *ES Energy & Environment*., **2019**, *3*(7), 25-44.
12. Shih, Y.-L.; Wu, C.-L.; Wu, T.-Y.; Chen, D.-H., Electrochemical fabrication of nickel phosphide/reduced graphene oxide/nickel oxide composite on nickel foam as a high performance electrode for supercapacitors. *Nanotechnology*., **2019**, *30*(11), 115601.
13. Padmanathan, N.; Selladurai, S.; Rahulan, K. M.; O'Dwyer, C.; Razeeb, K. M., NiO hybrid nanoarchitecture-based pseudocapacitor in organic electrolyte with high rate capability and cycle life. *Ionics*., **2015**, *21*, 2623-2631.
14. Ren, X.; Guo, C.; Xu, L.; Li, T.; Hou, L.; Wei, Y., Facile synthesis of hierarchical mesoporous honeycomb-like NiO for aqueous asymmetric supercapacitors. *ACS applied materials & interfaces*., **2015**, *7*(36), 19930-19940.
15. Alam, S. N.; Sharma, N.; Kumar, L., Synthesis of graphene oxide (GO) by modified hummers method and its thermal reduction to obtain reduced graphene oxide (rGO). *Graphene.,* **2017**, *6*(1), 1-18.
16. (a) Mateos, D.; Valdez, B.; Castillo, J.; Nedev, N.; Curiel, M.; Perez, O.; Arias, A.; Tiznado, H., Synthesis of high purity nickel oxide by a modified sol-gel method. *Ceramics International*., **2019**, *45*(9), 11403-11407; (b) Nalage, S.; Chougule, M.; Sen, S.; Joshi, P.; Patil, V., Sol–gel synthesis of nickel oxide thin films and their characterization. *Thin Solid Films*., **2012**, *520*(15), 4835-4840.
17. Yung, T.-Y.; Huang, L.-Y.; Chan, T.-Y.; Wang, K.-S.; Liu, T.-Y.; Chen, P.-T.; Chao, C.-Y.; Liu, L.-K., Synthesis and characterizations of Ni-NiO nanoparticles on PDDA-modified graphene for oxygen reduction reaction. *Nanoscale research letters*., **2014**, *9*, 1-6.
18. Kumar, R.; Singh, R. K.; Savu, R.; Dubey, P. K.; Kumar, P.; Moshkalev, S. A., Microwave-assisted synthesis of void-induced graphene-wrapped nickel oxide hybrids for supercapacitor applications. *RSC advances.,* **2016**, *6*(32), 26612-26620.

19. (a) Mohd Zaid, N. A.; Idris, N. H., Enhanced capacitance of hybrid layered graphene/nickel nanocomposite for supercapacitors. *Scientific reports.*, **2016**, *6*(1), 1-8; (b) Zhang, L.; Shi, G., Preparation of highly conductive graphene hydrogels for fabricating supercapacitors with high rate capability. *The Journal of Physical Chemistry C.*, **2011**, *115*(34), 17206-17212.
20. Li, W.; Bu, Y.; Jin, H.; Wang, J.; Zhang, W.; Wang, S.; Wang, J., The preparation of hierarchical flowerlike NiO/reduced graphene oxide composites for high performance supercapacitor applications. *Energy & fuels.,* **2013**, *27*(10), 6304-6310.
21. Xue, J.; Xu, H.; Wang, S.; Hao, T.; Yang, Y.; Zhang, X.; Song, Y.; Li, Y.; Zhao, J., Design and synthesis of 2D rGO/NiO heterostructure composites for high-performance electrochromic energy storage. *Applied Surface Science.*, **2021**, *565*, 150512.
22. Yan, J.; Fan, Z.; Sun, W.; Ning, G.; Wei, T.; Zhang, Q.; Zhang, R.; Zhi, L.; Wei, F., Advanced asymmetric supercapacitors based on Ni(OH)2/graphene and porous graphene electrodes with high energy density. *Advanced Functional Materials.*, **2012**, *22* (12), 2632-2641.